

This Provisional PDF corresponds to the article as it appeared upon acceptance.
Fully formatted PDF and full text (HTML) versions will be made available soon.

Visit Frontiers at: www.frontiersin.org

Substrate Arrays of Iridium Oxide Microelectrodes for *in vitro* neuronal interfacing

Shady Gawad^{1,2}, Michele Giugliano^{3,4}, Marc Heuschkel⁵, Borge Wessling⁶,
Henry Markram³, Uwe Schnakenberg⁶, Philippe Renaud¹, Hywel Morgan²

¹ Laboratory of Microsystems, Ecole Polytechnique Fédérale de Lausanne, Lausanne 1015, Switzerland.

² School of Electronics and Computer Science, University of Southampton, Southampton, UK

³ Laboratory of Neural Microcircuitry, Brain Mind Institute, Ecole Polytechnique Fédérale de Lausanne, Lausanne 1015, Switzerland.

⁴ Dept. of Biomedical Sciences, University of Antwerp, Universiteitsplein 1, B-2610 Wilrijk, Belgium.

⁵ Ayanda Biosystem SA, Parc Scientifique, PSE, Ecole Polytechnique Fédérale de Lausanne, Switzerland.

⁶ Inst. for Materials in Electrical Eng. I, RWTH Aachen University, Sommerfeldstr. 24, D-52074 Aachen.

Abstract (250 words max, now 240)

The design of novel bidirectional interfaces for *in vivo* and *in vitro* nervous systems is an important step towards future functional neuroprosthetics. Small electrodes, structures and devices are necessary to achieve high-resolution and target-selectivity during stimulation and recording of neuronal networks, while significant charge transfer and large signal-to-noise ratio are required for accurate time resolution. In addition, the physical properties of the interface should remain stable across time, especially when chronic *in vivo* applications or *in vitro* long-term studies are considered, unless a procedure to actively compensate for degradation is provided.

In this short report, we describe the use and fabrication of arrays of 120 planar microelectrodes (MEAs) of sputtered Iridium Oxide (IrOx). The effective surface area of individual microelectrodes is significantly increased using electrochemical activation, a procedure that may also be employed to restore the properties of the electrodes as required. The electrode activation results in a very low interface impedance, especially in the lower frequency domain, which was characterized by impedance spectroscopy. The increase in the roughness of the microelectrodes surface was imaged using digital holographic microscopy and electron microscopy. Aging of the activated electrodes was also investigated, comparing storage in saline with storage in air.

Demonstration of concept was achieved by recording multiple single-unit spike activity in acute brain slice preparations of rat neocortex. Data suggests that extracellular recording of action potentials can be achieved with planar IrOx MEAs with good signal-to-noise ratios..

Keywords

substrate microelectrodes; extracellular recordings; electrophysiology; impedance spectroscopy; neurons; cortex

1. Introduction

A number of reports, documenting the use of IrOx microelectrodes for neuroengineering and biomedical applications, have been recently presented in the literature. The interest in this material is driven by its excellent properties as a functional coating for implantable stimulation electrodes, with applications in stimulating/recording heart, neuronal or retinal tissues (Mokwa 2007; Cogan, 2006; Marzouk *et al.*, 1998; Blau *et al.*, 1997). High-resolution electrical stimulation and recording directly benefits from miniaturization of the electrodes, whilst retaining a high and reversible charge capture and delivery capacity (Wessling *et al.*, 2006; Cogan *et al.*, 2005). Although electrode coating with nanoparticles demonstrates excellent performances both in stimulation (Mazzatenta *et al.*, 2007) and recording (Keefer *et al.*, 2008; Gabriel *et al.*, 2008; Gabay *et al.*, 2007), the regenerative electrical activation of IrOx electrodes is simpler and faster than nanotechnological fabrication or deposition processes.

In applications requiring extracellular recordings, the efficiency of the charge-delivery capacity of the electrodes material is of lower priority. However, low impedance and long-term stability of the interface is an important requirement and IrOx electrodes provide both of these requirements. . This short paper will examine and discuss the use of arrays of activated IrOx electrodes, and their use for short-term *in vitro* extracellular recording of neuronal electrical activity. We report preliminary results employing neocortical acute tissue slices of the rat brain, selected as a target example to characterise IrOx electrode ageing and the recording of weak spontaneous electrical activity (Egert *et al.*, 2002). In this context, *in vitro* simultaneous multisite recording of the spontaneous and evoked electrical activity of the nervous system represent an important step towards the understanding of the network-level and single-cell correlates of many (patho)physiological mechanisms (Rinaldi *et al.*, 2007; Silberberg and Markram, 2007), as well as a crucial requirement for the validation of large-scale mathematical models and theories of the brain (Traub *et al.*, 2005; Markram, 2006).

2. Materials and Methods

2.1. IrOx Microelectrodes Arrays

Microelectrode arrays (MEAs) were fabricated in clean rooms at the Institute of Microtechnique of the EPFL and Institute of Electrical Engineering I at RWTH Aachen University, through a custom technological process (Figure 1). Briefly, a reversal photoresist lift-off technique (AZ5214, Clariant, Germany) was employed to pattern metal using a glass substrate. The iridium layer was sputter-deposited as described in Wesslig *et al.*, (2007), with the following parameters: 180 W – DC Power, 100sccm – Argon flow and 10.4 sccm – oxygen flow. A layer of photosensitive SU-8 (5 μm) was finally used as an insulating layer (Lorenz *et al.*, 1997), covering the iridium leads while leaving free access to the electrodes sites and contacts (Figure 1a).

The MEA layout consisted in a 12×10 square grid arrangement of 120 circular microelectrodes, each measuring 30 μm in diameter and located 100 μm apart from each other (Figure 2b). MEAs were glued onto printed circuit boards (PCB - Figures 1b, 2) by a screen-printing technique, to provide external interfacing to multichannel amplifying electronics (Figure 2a). Platinum-based MEAs, with identical layout and electrode geometry, were also fabricated (Nam *et al.*, 2006), and employed for comparison. Finally, the recording chamber was sealed with epoxy and silicone sealant (e.g. Sylgard 184, Distrelec, Switzerland) to ensure watertight connection of the MEA (Fig. 1b).

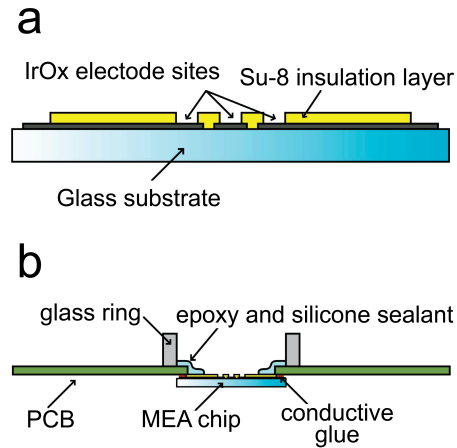


Figure 1: Cross-section of a microelectrode array (a), showing the substrate, metal and insulation layers (SU-8 epoxy). The MEA is assembled to a printed circuit board (PCB) that allows signal interfacing for amplification and data acquisition (b). Glass substrates are glued under the PCB with conductive materials, providing contacts to the PCB tracks. Finally, a glass ring was mounted on the top of the MEA using an epoxy/silicone sealant, defining a watertight recording chamber.

2.2. Preparation of brain slices and pharmacology

Brain slices (300 μm thick) were prepared from Wistar rats, on postnatal days 15-20, by standard procedures (Köndgen *et al.*, 2008), in accordance with institutional and national guidelines (Cantonal Veterinary Service, license n. 1550.1 to M.G.). Briefly, brains were quickly excised and rinsed in ice-cold ($<4^{\circ}\text{C}$) artificial cerebrospinal fluid (aCSF; containing in mM: 125 NaCl, 25 NaHCO_3 , 2.5 KCl, 1.25 NaH_2PO_4 , 2 CaCl_2 , 1 MgCl_2 , 25 glucose, continuously bubbled with 95% O_2 , 5% CO_2). Parasagittal neocortical slices were cut with a vibratome (VT1000S; Leica Microsystems, Wetzlar, Germany), trimmed down to an area of about $3 \times 2 \text{ mm}^2$ centered to the primary somatosensory area (S1), and incubated at 35°C for 45 min. Slices were afterward left at room temperature (24°C). Electrophysiological recordings were carried out at room temperature, perfusing slices with an extracellular solution that differed from the aCSF in the concentration of potassium, calcium and magnesium ions (i.e. 6.25 KCl, 1.5 CaCl_2 , 0.5 MgCl_2 , bubbled with 95% O_2 , 5% CO_2). This results in an increase of the basal level of spontaneous electrical activity, as in Berger *et al.*, (2006) (see also Richardson *et al.*, 2005). In some experiments, NMDA (N-methyl-D-aspartic acid, 10-100 μM) was applied to mimic the non-selective activation of glutamatergic NMDA-receptors and further probe network-level excitability. All the chemicals were obtained from Sigma-Aldrich or Merck (Switzerland).

2.3. Surface coating of the MEAs

MEAs were used repeatedly and cleaned before each experiment with methanol and distilled water. To improve mechanical adhesion of the tissue slice, the MEA surfaces was routinely coated with cellulose nitrate (CN, Schleicher & Schuell, Dassel, Germany) dissolved in methanol (0.14 mg/ml). 4-6 μl of this solution was spread out around the electrode area and dried in air. A glass ring (diameter 20 mm), glued to the PCB base plate with silicone rubber (Sylgard 184, World Precision Instruments, Berlin, Germany), formed a recording chamber with a volume of 1.5 ml.

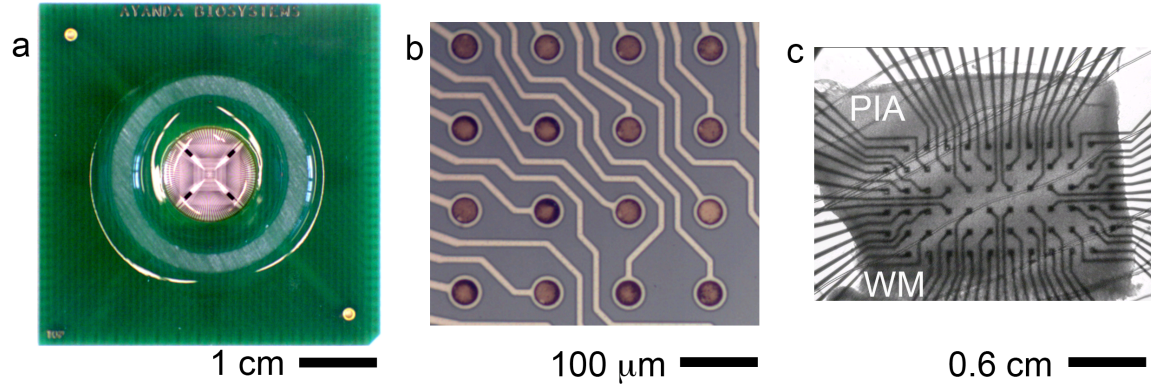


Figure 2: Top view of the full MEA assembled on a PCB (a) and close-up of the substrate electrode array (top-left corner) (b), showing 16 electrode sites and the insulated leads. Each microelectrode is $30\ \mu\text{m}$ in diameter, with a $100\ \mu\text{m}$ spacing, arranged in a 12×10 square grid layout. A brain tissue slice (c), obtained acutely from the somatosensory rat cortex and comprising cellular layers between the *pia* and the *white matter* (WM), can be mechanically coupled to the MEA to record and stimulate the neuronal electrical activity (see Fig. 6).

3. Results

3.1. Iridium activation process

IrOx microelectrodes were activated and restored to the activated state using a simple electrical protocol: each MEA electrode was connected to a potentiostat (AUTOLAB PGSTAT302, Echochemie, The Netherlands), with the counter and the reference terminals connected to a small platinum plate electrode, dipped into the phosphate buffer solution (PBS 10mM phosphate buffer, 2.7mM KCl and 137mM NaCl, pH 7.4 at 25°C, Sigma-Aldrich, Germany) with a contact surface of a few square millimeters. The MEA electrodes were used as the working electrodes (Bockris *et al.*, 2000). For the sake of simplicity, all 120 electrodes were activated simultaneously by connecting them in parallel rather than using a long and tedious but more controlled serial process. This approach, may however, lead to an inhomogeneous current density, so that the degree of activation would differ from one electrode to another.

In order to study the activation, as well as the effects of aging and reactivation, a number of linear voltage sweep cycles were performed until the peak current at the sweep maximum and minimum voltage no longer increased from one cycle to the next. Four or five cycles, from 1.4 V to -1.4 V were found necessary to achieve this condition and thence surface activation. A number of trials were required to achieve successful activation and reproducible results. After 1 or 2 cycles, micrometer sized bubbles could occasionally form on top of the electrodes as the relatively high voltage used caused electrolysis of water. Since these bubbles were found to partially mask or shield the electrodes from the electrolyte, a small plastic needle was used to establish a liquid flow on top of the electrode surface and detach the bubbles, allowing the electrode activation process to resume. In addition, because of the platinum counter/reference electrode properties, the measured sweep current was sometimes asymmetric. In order to prevent this effect a DC voltage offset (up to 0.2 V) was used to compensate for activation currents that were too large in magnitude.

After (re)activation, the electrode arrays were rinsed carefully in PBS solution and the electrode impedance characterized using a precision impedance analyzer (4294A, Agilent, USA).

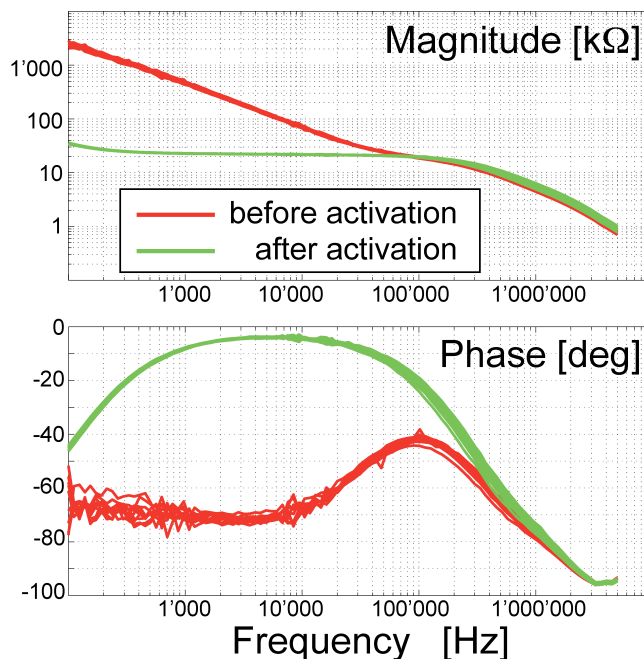


Figure 3: Electrochemical impedance spectroscopy was performed on sets ($n = 10$) of micro electrodes. Measurements were performed in PBS, with a conductivity adjusted to 12,800 S/cm with deionized water before and after activation. The plots show the magnitude (**upper panel**) and the phase (**lower panel**) of the impedance of the electrode-electrolyte interface, over the frequency range from 100 Hz to 5 MHz (100

sample points), with 50 mV modulation amplitude. After MEA activation, the charge transfer properties are greatly improved, changing the filter-properties from a high-pass to an all-pass in the low frequency range.

The results of the activation protocols are summarized in Figure 3, where the characteristic frequency of the electrode double layer impedance decreases by 3 orders of magnitude compared to inactivated electrodes (taken at 45° phase point), from 10^5 to 10^2 Hz. The impedance homogeneity was also found to be very high, with differences only at higher frequencies probably resulting from stray capacitances in the leads rather than from heterogeneity in electrode surface properties.

Aging of the electrode impedance properties was determined by measuring the impedance after 48 hours, with electrodes stored in PBS or dry (Figure 4). Storing MEAs in a dry environment leads to a small increase in phase and impedance, by only a few percents. As expected, the electrode impedance reduced with time when MEAs were stored in PBS. After reactivation with 1 or 2 activation cycles, the original properties of the electrodes could be recovered.

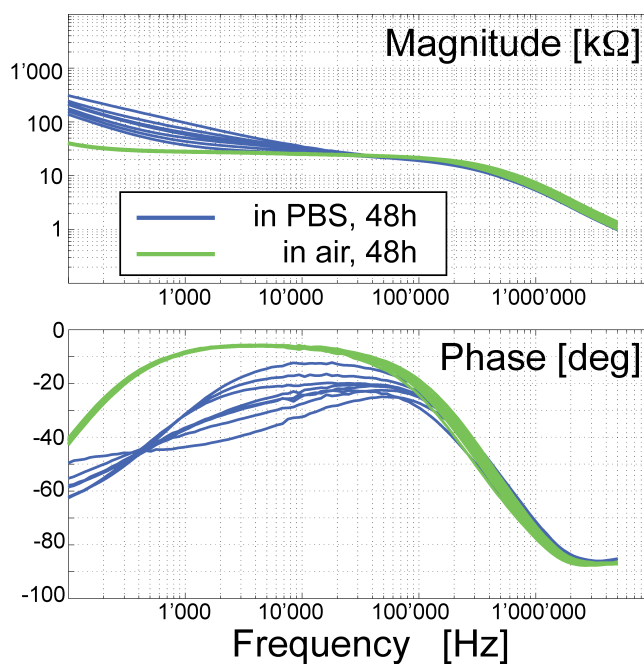


Figure 4: Electrochemical impedance spectroscopy (as in Figure 3), for MEAs stored dry or in PBS for 48 hours. The substantial decrease in the impedance magnitude resulting from the activation process (compare to Figure 3, top panel) was partly lost for electrodes ($n = 8$) stored in PBS. On the other hand, electrodes stored in air ($n = 10$), showed an unchanged profile after 48 hours.

3.2. Electrode Imaging

To further characterize the activation and aging effects of IrOx MEAs, topographic images were acquired using a digital holographic microscope capable of resolving vertical surface roughness in the nm range (DHM R1000, Lyncée Tec SA, Switzerland). In this technique the in-plane resolution is still limited by diffraction, and was in the sub-micrometer range (Montfort *et al.*, 2006).

As shown in Figure 5a-c, after digital reconstruction, the hologram of the electrode surface shows that the increase in roughness induced by activation is still present after 1 month of storage in dry conditions. For electrodes stored in saline, the surface had returned to an intermediate state, consistent with data in figure 4. Panel (d) of Figure 5 shows scanning electron microscopy images, indicating that the activated IrOx surface has nanometer scale roughness details.

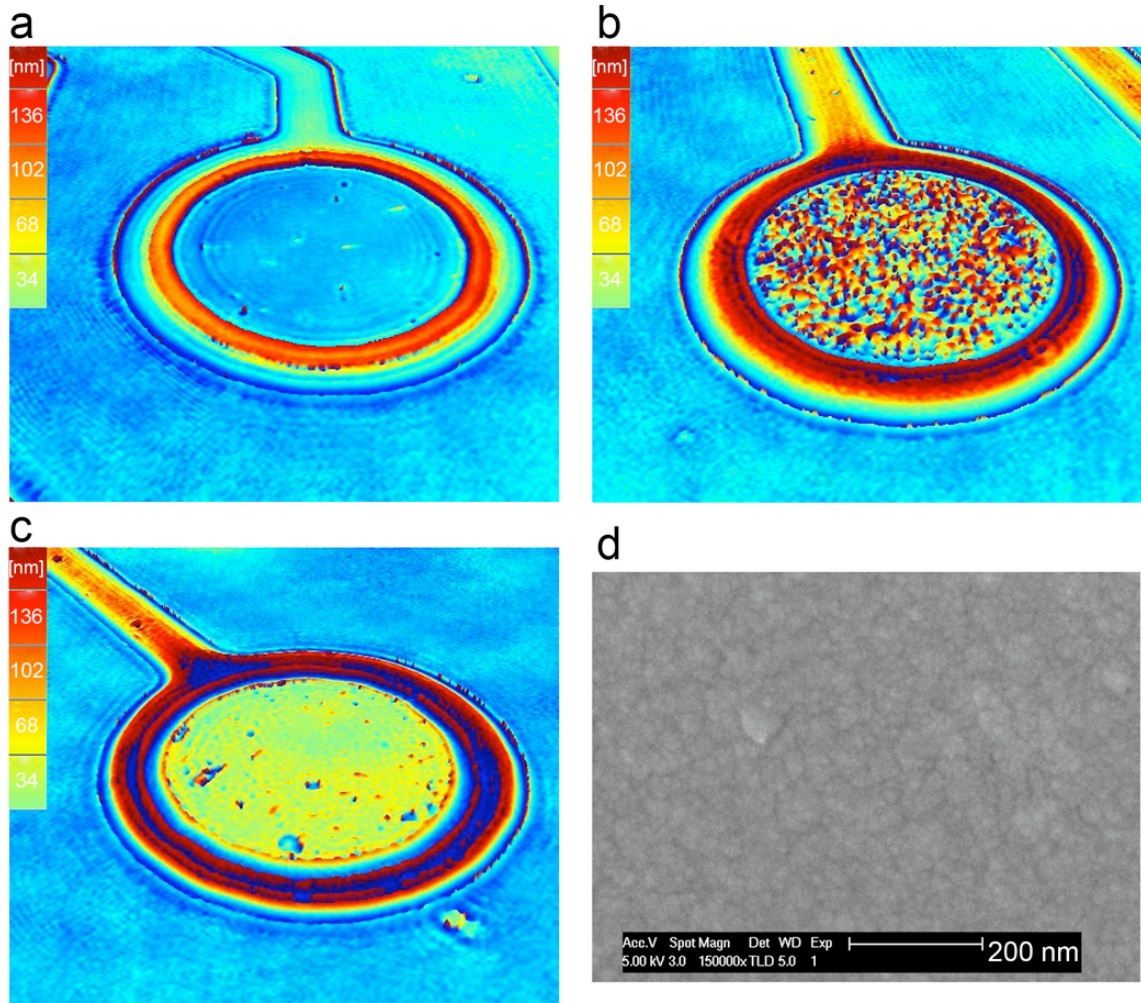


Figure 5: The surface roughness of MEAs, before and after IrOx activation, studied by digital holographic microscopy (a-c) and scanning electron microscopy (d). The first technique reveals a substantial difference in the vertical nanometer scale surface roughness following IrOx activation (**b**), compared to electrode surface before activation (**a**). Panel **b** shows an image of an electrode after 1 month of storage in air, whilst electrodes stored for 1 month in PBS (**c**) degenerate and return to a condition intermediate between **a** and **b**. Scanning electron microscopy shows the nanometer scale surface roughness of an activated electrode (**d**).

3.3. Noise characterization

Noise analysis was performed on the raw voltage traces, recorded in sets of 5, obtained with the electrolyte used in the electrophysiological experiments (i.e. aCSF – see Methods). Although the A/D 12-bits conversion resolution (i.e. 0.052 V/level) used for detecting neuronal activity was just able to resolve the very small signal-amplitude of the noise in IrOx electrodes, the distribution of the amplitudes was Gaussian, with a standard deviation of 0.66 V (for 181 planar IrOx electrodes). These excellent features can be compared to arrays of platinum microelectrodes, fabricated using an identical process and layout. The same noise analysis performed on these MEAs had 10-times worse performances (i.e. 5.7 V, across 123 planar Pt electrodes).

3.4. Electrophysiological recordings and analysis

Neuronal spiking activity was recorded extracellularly using the IrOx integrated thin-film MEAs as in (Egert et al., 2002). Slice alignment to the inner area of the MEA was performed manually under visual control, making each of the six cortical layers cover the electrodes.

After 5 min of accommodation time following the mounting of each slice on the MEAs, spiking activity was monitored and recorded for 30min. Signals from each electrode were amplified (1200 times) and band-pass filtered (300-3000Hz) with a 120-channels amplifier (Ayanda Biosystems SA, Lausanne, Switzerland). Raw signals were further sampled at 25kHz/channel from 120 channels simultaneously, and digitized (12-bit) through a 128-channel PCI-bus A/D card (Multi Channel Systems, Reutlingen, Germany) for off-line analysis. MCRack (Multichannel Systems, Reutlingen, Germany) was used to acquire and store the data (2Gb/session). Data were analyzed using Matlab (The Mathworks, Natick - MA, USA) and custom software written in C. Raw data were digitally conditioned using second order Butterworth filters 150Hz and 2.5kHz and fully rectified. The occurrence of an action potential was identified by a peak-detection algorithm, based on the crossing of an adaptive threshold (i.e. the LimAda algorithm of Wagenaar et al., 2006). Recorded events included the time-stamp of the spike, the index of the corresponding electrode, and the preceding 2ms and following 4ms of the corresponding voltage trace (Figure 6b). The conclusions reported here are based on repeated observations collected by MEAs on 6 cortical tissue slices.

Figure 6 is a sample of a recording, showing extracellular voltages recorded from a few IrOx electrodes. As discussed in the previous section, the good signal-to-noise ratio translates to a substantially higher probability of detecting single-unit activity in acute slices of rat neocortex. As discussed in Martinoia *et al.*, (2004), single-unit events resemble higher time-derivative of an intracellular action potentials, consistent with the electrical properties reported in Figure 3. In preliminary results we found that IrOx MEAs detected more spontaneous activity than Pt-MEAs, although a more accurate quantitative comparison requires the same brain tissue slice to be removed from one MEA and mounted on another. Such a procedure was mechanically stressful for the tissue and it was not pursued in this study.

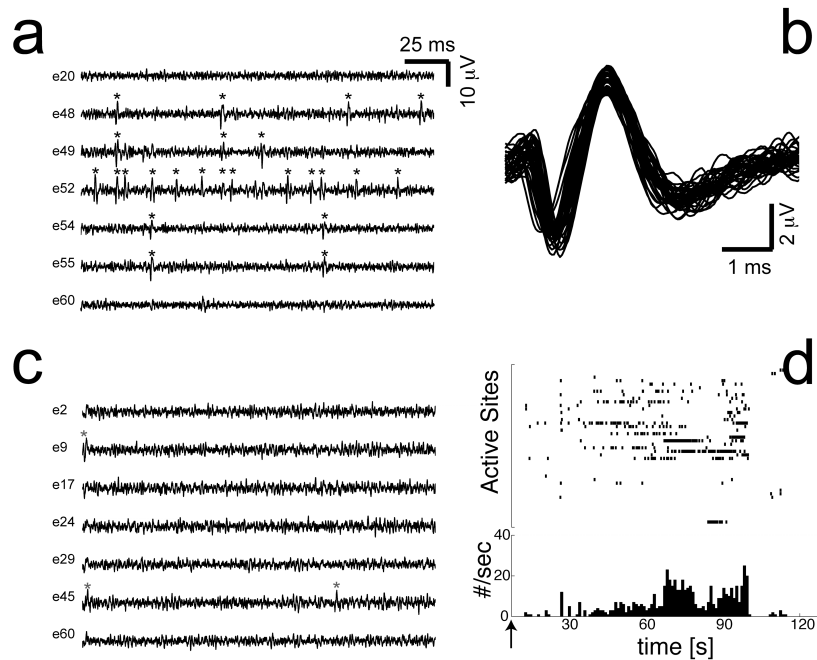


Figure 6: Extracellular voltages, recorded from IrOx electrodes (a), demonstrates excellent signal-to-noise ratio in probing spontaneous spiking activity in acute slices of rat neocortex. Asterisks identify the occurrence of single-unit events, whose waveforms (b) resemble the second-derivative of an intracellular

action potential, consistent with the expected behavior of the neuron-electrode electrochemical interface. (c) Due to a higher intrinsic noise, planar platinum MEAs allow only the detection of strong signals and generally transduce less neuronal activity. Transient collective network responsiveness to bath application of an agonist of glutamatergic excitatory synaptic receptors (i.e. NMDA_R), occurred at the time indicated by the arrow, and were simultaneously monitored by the IrOx MEAs electrodes (d): Once detected by an adaptive-threshold peak-detection algorithm, spikes from individual electrodes are represented by the time of occurrence (**top panel**) or by the overall event rate, specified in bins of 1 second (**bottom panel**).

4. Discussion

The extracellular spontaneous spiking activity level measured using the activated IrOx MEAs demonstrate that good results can be achieved with these planar electrodes. In general, for similar signal-to-noise ratios, 3D electrodes or platinum black electrodes have been proposed (Heuschkel *et al.*, 2002), although at the cost of more complicated manufacturing process (3D devices) and less reproducible results (platinum black). The high reproducibility of the IrOx impedance data across the array (Figures 3-4) is due to the fact that the activation process self-limits because the current density saturates after a number of cycles. Electrodeposition of Pt-black is influenced by the distribution and the current density at the electrode surface, which varies from one electrode to another as well as during the deposition process through changes of electrode surface geometry. In addition, electrodeposition of Pt black on 120 electrodes MEAs is particularly challenging and time consuming as it requires on-line monitoring of individual currents at each electrode throughout the entire deposition process.

The storage of the IrOx electrodes in dry conditions showed that electrode properties can be preserved. On the other hand, although a reactivation process is possible, electrode degradation is considerable in PBS.

Although the study degradation process would deserve more attention, it is likely that such an electrode aging is due to the IrOx returning to a lower oxidation level thus decreasing its effective surface, as its observed correlates are fully reversible. The electrical reactivation process is not compatible with the presence of biological samples, which makes the quality of long-term monitoring (over 48h) dependent on the electrode ageing.

Nevertheless, measurements over shorter time windows, particularly useful in slice electrophysiology, can be achieved with acceptable electrode properties. In such a case, the array can be then daily reactivated and cleaned a number of times, to restore the original electrode properties, reusing the same MEAs a number of times.

Acknowledgements

The authors are grateful to S. Garcia for excellent lab assistance and to L. Gambazzi for discussions. S.G. is grateful to E. Cucho for assistance with digital holographic microscopy and A. Tourvieille for assistance with scanning electron microscopy. M.G. and H.M. acknowledge support from the EPFL and the European Commission "NEURONANO" FP6 grant (NMP4-CT-2006-031847).

Conflict-of-Interest Statement

The authors declare that the research was conducted in the absence of any commercial or financial relationships that could be construed as a potential conflict of interest.

References

- Berger, T., Lüscher, H.-R., and Giugliano, M. (2006). Transient rhythmic network activity in the somatosensory cortex evoked by distributed input in vitro. *Neurosci.* 140:1401-1413.
- Blau, A., Ziegler, C., Heyer, M., Endres, F., Schwitzgebel, G., Matthies, T., Stieglitz, T., Meyer, J.U., and Gopel, W. (1997). Characterization and optimization of microelectrode arrays for in vivo nerve signal recording and stimulation. *Biosens. Bioelec.* 12:883-892.
- Bockris, J.O'M., Reddy, A.K.N., and Gamboa-Aldeco, M. (2000) Modern Electrochemistry 2A: Fundamentals of Electrode Processes, 2nd ed., Kluwer Academic / Plenum Publishers, New York.

Cogan, S.F. (2006). *In vivo* and *In vitro* differences in the charge-injection and electrochemical properties of iridium oxide electrodes. *Proc. of IEEE 28th Intl. Conf. Eng, in Med. Biol. Soc. - EMBS*, 882-885.

Cogan, S.F., Troyk, P.R., Ehrlich, J., and Plante, T.D. (2005). *In vitro* comparison of the charge-injection limits of activated iridium oxide (AIROF) and platinum-iridium microelectrodes. *IEEE Transactions on Biomed. Eng.* 52:1612-1614.

Egert, U., Heck, D., and Aertsen, A. (2002). Two-dimensional monitoring of spiking networks in acute brain slices. *Exp. Brain Res.* 142:268-274.

Gabay, T., Ben-David, M., Kalifa, I., Sorkin, R., Abrams, Z., Ben-Jacob, E., and Hanein, Y. (2007) Electro-chemical and biological properties of carbon nanotube based multi-electrode arrays. *Nanotech.* 18(3):035201-035207.

Gabriel, G., Gómez-Martínez, R., Villa, R. (2008) Single-walled carbon nanotubes deposited on surface electrodes to improve interface impedance. *Physiol. Measurm.* 29(6): S203-S212.

Heuschkel, M.O., Fejtl, M., Raggenbass, M., Bertrand, D., and Renaud, P. (2002). A three-dimensional multi-electrode array for multi-site stimulation and recording in acute brain slices. *J. Neurosci. Methods.* 114(2):135-148.

Keefer, E.W., Botterman, B.R., Romero, M.I., Rossi, A.F., and Gross, G.W. (2008). Carbon nanotubes coating improves neuronal recordings. *Nat. Nanotech.* 3(7):434-439.

Köndgen H, Geisler C, Fusi S, Wang XJ, Lüscher HR, Giugliano M. (2008) The Dynamical Response Properties of Neocortical Neurons to Temporally Modulated Noisy Inputs In Vitro. *Cereb. Cortex*, in press.

Lorenz H, Despont M, Fahrni N, LaBianca N, Renaud P, Vettiger P (1997) SU-8: a low-cost negative resist for MEMS. *J Micromech Microeng* 7:121-4.

Markram, H. (2006). The Blue Brain Project. *Nat. Rev. Neurosci.* 7:153-160.

Marzouk, S.A., Ufer, S., Buck, R.P., Johnson, T.A., Dunlap, L.A., and Cascio, W.E. (1998). Electrodeposited iridium oxide pH electrode for measurement of extracellular myocardial acidosis during acute ischemia. *Anal. Chem.* 70:5054-5061.

Martinoia, S., Massobrio, P., Bove, M., Massobrio, G. (2004). Cultured neurons coupled to microelectrode arrays: circuit models, simulations and experimental data. *IEEE Trans. Biomed. Eng.* 51(5):859-864.

Mazzatenta, A., Giugliano, M., Campidelli, S., Gambazzi, L., Businaro, L., Markram, H., Prato, M., and Ballerini, L. (2007). Interfacing neurons with carbon nanotubes: electrical signal transfer and synaptic stimulation in cultured brain circuits. *J. Neurosci.* 27(26):6931-6936.

Montfort, F., Colomb, T., Charrière, F., Kühn, J., Marquet, P., Cuche, E., Herminjard, S., and Depeursinge, C. (2006). Submicrometer optical tomography by multiple-wavelength digital holographic microscopy. *Appl Opt.* 45(32):8209-17.

Mokwa, W. (2007). Artificial Retinas, in: *Comprehensive Microsystems Vol. 3*, Gianchandani, Tabata, Zappe, eds., Elsevier.

Nam, Y., Wheeler, B.C., Heuschkel, M.O. (2006). Neural recording and stimulation of dissociated hippocampal cultures using microfabricated three-dimensional tip electrode array. *J. Neurosci. Methods* 155(2):296-299.

Richardson, M.J., Melamed, O., Silberberg, G., Gerstner, W., and Markram, H. (2005) Short-term synaptic plasticity orchestrates the response of pyramidal cells and interneurons to population bursts. *J. Comp. Neurosci.* 18(3):323-331.

Rinaldi, T., Silberberg, G., and Markram, H. (2007). Hyperconnectivity of Local Neocortical Microcircuitry Induced by Prenatal Exposure to Valproic Acid. *Cereb. Cortex* 18(4):763-70.

Silberberg, G., and Markram, H. (2007). Disynaptic inhibition between neocortical pyramidal cells mediated by Martinotti cells. *Neuron* 53:735-746.

Traub, R., Contreras, D., and Whittington, M. (2005). Combined experimental/simulation studies of cellular and network mechanisms of epileptogenesis *in vitro* and *in vivo*. *J. Clin. Neurophysiol.* 22:330-342.

Wagenaar DA, Pine J, Potter SM (2006) An extremely rich repertoire of bursting patterns during the development of cortical cultures. *BMC Neurosci* 7:11.

Wessling, B., Mokwa, W., and Schnakenberg, U. (2006). RF-sputtering of iridium oxide to be used as stimulation material in functional medical implants. *J. Micromech. Microeng.* 16:S142-S148.

Wessling, B., Besmehn, A., Mokwa, W., and Schnakenberg, U. (2007). Reactively sputtered iridium oxide influence of plasma excitation and substrate temperature on morphology, composition, and electrochemical characteristics. *J. Electrochem. Soc.* 154:F83-F89.